

# NMR Spectroscopy of Phosphorylated Wild-Type Rhodopsin: Mobility of the Phosphorylated C-Terminus of Rhodopsin in the Dark and upon Light Activation<sup>†</sup>

Elena Getmanova,<sup>‡</sup> Ashish B. Patel,<sup>§</sup> Judith Klein-Seetharaman,<sup>||</sup> Michele C. Loewen,<sup>‡</sup> Philip J. Reeves,<sup>‡</sup> Noga Friedman,<sup>⊥</sup> Mordechai Sheves,<sup>⊥</sup> Steven O. Smith,<sup>§</sup> and H. Gobind Khorana<sup>\*:‡</sup>

Department of Biology, Massachusetts Institute of Technology, Cambridge, Massachusetts 02139, Departments of Physiology and Biophysics, Biochemistry and Cell Biology, Center for Structural Biology, State University of New York–Stony Brook, Stony Brook, New York 11794-5115, Department of Pharmacology, University of Pittsburgh School of Medicine, Pittsburgh, Pennsylvania 15261, and Department of Organic Chemistry, Weizmann Institute of Science, Rehovot, Israel

Received May 12, 2003; Revised Manuscript Received October 23, 2003

**ABSTRACT:** Binding of arrestin to light-activated rhodopsin involves recognition of the phosphorylated C-terminus and several residues on the cytoplasmic surface of the receptor. These sites are in close proximity in dark, unphosphorylated rhodopsin. To address the position and mobility of the phosphorylated C-terminus in the active and inactive receptor, we combined high-resolution solution and solid state NMR spectroscopy of the intact mammalian photoreceptor rhodopsin in detergent micelles as a function of temperature. The <sup>31</sup>P NMR resonance of rhodopsin phosphorylated by rhodopsin kinase at the C-terminal tail was observable with single pulse excitation using magic angle spinning until the sample temperature reached  $-40\text{ }^{\circ}\text{C}$ . Below this temperature, the <sup>31</sup>P resonance broadened and was only observable using cross polarization. These results indicate that the phosphorylated C-terminus is highly mobile above  $-40\text{ }^{\circ}\text{C}$  and immobilized at lower temperature. To probe the relative position of the immobilized phosphorylated C-terminus with respect to the cytoplasmic domain of rhodopsin, <sup>19</sup>F labels were introduced at positions 140 and 316 by the reaction of rhodopsin with 2,2,2-trifluoroethanethiol (TET). Solid state rotational-echo double-resonance (REDOR) NMR was used to probe the internuclear distance between the <sup>19</sup>F and the <sup>31</sup>P-labels. The REDOR technique allows <sup>19</sup>F•••<sup>31</sup>P distances to be measured out to  $\sim 12\text{ }\text{Å}$  with high resolution, but no significant dephasing was observed in the REDOR experiment in the dark or upon light activation. This result indicates that the distances between the phosphorylated sites on the C-terminus and the <sup>19</sup>F sites on helix 8 (Cys 316) and in the second cytoplasmic loop (Cys140) are greater than  $12\text{ }\text{Å}$  in phosphorylated rhodopsin.

The visual photoreceptor rhodopsin is a member of the large family of G protein-coupled receptors. These receptors have a common architecture consisting of seven transmembrane helices. Activation of rhodopsin by light is initiated by isomerization of the photoreactive 11-*cis*-retinylidene chromophore. The chromophore is covalently bound within the bundle of transmembrane helices through a protonated Schiff base linkage to Lys 296. Rigid-body motion of the transmembrane helices couples retinal isomerization to conformational changes in the cytoplasmic loops of rhodopsin, resulting in receptor activation.

Phosphorylation of light-activated rhodopsin by rhodopsin kinase is the first step in desensitization of the receptor. Serines at positions 338 and 343 are established to be the preferential sites of phosphorylation *in vitro* (1–3) (Figure 1). Arrestin recognizes the phosphates on the C-terminus of rhodopsin and subsequently binds to the cytoplasmic surface

and inactivates the receptor. Asn73, at the end of transmembrane helix 2, as well as Pro142 and Met143 in the second cytoplasmic loop, have been shown to be particularly important for arrestin binding (4). It is likely that the specific conformation of the cytoplasmic loops and the C-terminus of the phosphorylated, light-activated rhodopsin provides the binding specificity for arrestin.

Recently, it has been shown that specific mutants of arrestin, but not wild-type protein, can bind to phosphorylated dark rhodopsin and unphosphorylated light-activated rhodopsin (5). Binding of the C-terminal phosphates of rhodopsin is thought to break a buried salt bridge in arrestin that constrains arrestin in an inactive (low affinity) conformation. (The mutations destabilize the inactive arrestin structure.) Activated arrestin then tightly binds rhodopsin by recognizing specific loop residues that are exposed upon light activation. This raises the question about the proximity of the phosphorylation sites with other residues involved in arrestin binding in phosphorylated rhodopsin in the inactive (dark) and active (light) conformations.

The recent crystal structure of the dark state of rhodopsin has provided considerable insights into the conformation of the inactive, unphosphorylated receptor (6, 7). While the  $2.6\text{ }\text{Å}$  structure clearly defines the position of the retinal

<sup>†</sup> This research was supported by National Institutes of Health Grant NEI11716 (H.G.K.) and at Stony Brook by the National Institutes of Health (S.O.S. GM-41412), the National Science Foundation under Instrumentation Grant No. 9907840, and the W. M. Keck Foundation.

<sup>‡</sup> Massachusetts Institute of Technology.

<sup>§</sup> State University of New York–Stony Brook.

<sup>||</sup> University of Pittsburgh School of Medicine.

<sup>⊥</sup> Weizmann Institute of Science.

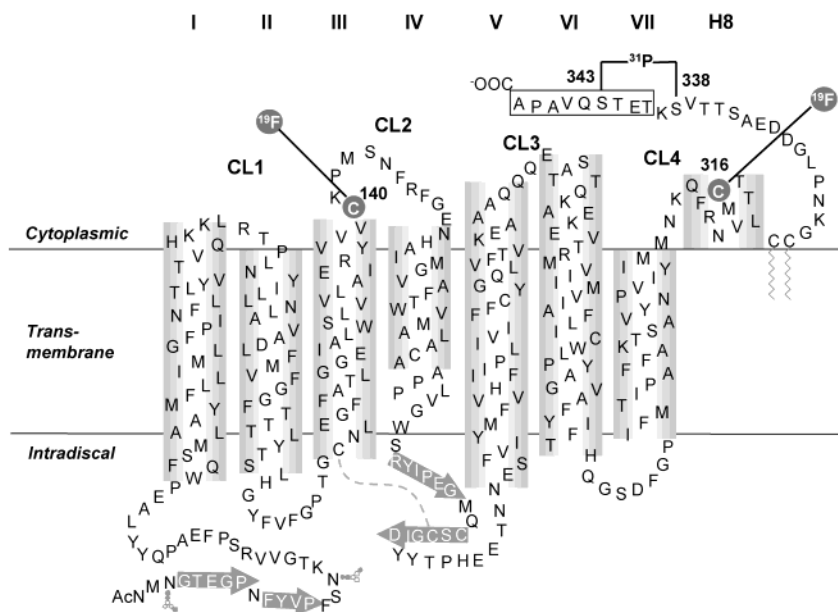


FIGURE 1: Secondary structure model based on the crystal structure of rhodopsin showing positions of the <sup>19</sup>F-labels and presumed phosphorylation sites in the C-terminus. Fluorine labels were introduced in cysteines at positions 140 and 316 in the cytoplasmic domain by derivatization with TET (Materials and Methods). Phosphate groups were introduced by phosphorylation of rhodopsin with endogenous rhodopsin kinase, presumably at the preferential phosphorylation sites (Ser338 and Ser343) at the C-terminus of rhodopsin (Materials and Methods). The C-terminal peptide sequence, which serves as the 1D4 antibody epitope, is boxed.

chromophore and the transmembrane helices, critical segments of the cytoplasmic regions, in particular of the C-terminus, are not well-resolved due to disorder or high flexibility in the protein crystal. Solution NMR<sup>1</sup> spectroscopy of full-length rhodopsin containing a <sup>15</sup>N-label at the backbone nitrogen of Lys339 in detergent micelles further suggests that the C-terminus is very flexible (8). Because of the difficulties in the interpretation of density for the C-terminus in the crystal structure, modeling has been restricted to the backbone atoms of residues 334–348 (6, 7). In the current structural model of rhodopsin, the C-terminus folds back toward the center of the helical bundle, bringing the two major phosphorylation sites, Ser338 and Ser343, into close proximity with the tertiary structure formed by helix 8, the ends of helices 1 and 2, and their connecting loop. In particular, Cys316 on helix 8 interacts closely with His65 in the first cytoplasmic loop and with Asn73 at the end of helix 2, both in solution (9) and in the crystal structure (6, 7). This indicates that in the absence of phosphorylation, the C-terminus interacts with the cytoplasmic domain in the region defined by helix 8 and the ends of helices 1 and 2.

To address the structure and interactions of the C-terminus of phosphorylated, light-activated rhodopsin, ideally a high-resolution crystal structure is needed. Such a structure is currently not amenable to protein crystallography. We have therefore taken advantage of an alternative approach that allows us to directly probe the distances of the major phosphorylation sites at the C-terminus of rhodopsin with respect to the two key areas that have been implicated in

arrestin binding (see above). This approach involves solid state NMR measurements of <sup>31</sup>P–<sup>19</sup>F distances using the <sup>31</sup>P nucleus of the phosphate groups and the incorporation of <sup>19</sup>F nuclei at native cysteines near the arrestin binding site. We have previously demonstrated the ability to introduce <sup>19</sup>F into specific cysteine residues in the cytoplasmic loops of rhodopsin by reaction with 2,2,2-trifluoroethanethiol (TET) (10). The two native cysteines in the cytoplasmic loops, Cys140 and Cys316, can be labeled quantitatively and exhibit resolved <sup>19</sup>F chemical shifts by solution NMR of rhodopsin in detergent micelles. Importantly, Cys316 is a direct neighbor of Asn73, and Cys140 is adjacent to Pro142/Met143, the critical residues involved in arresting binding. In this paper, we phosphorylate the C-terminus of rhodopsin using rhodopsin kinase and then derivatize Cys140 and Cys316 using TET. This provides unique <sup>19</sup>F and <sup>31</sup>P labels in the cytoplasmic loops and on the C-terminal tail of rhodopsin, respectively, that can be used in heteronuclear <sup>31</sup>P–<sup>19</sup>F distance measurements using rotational echo double resonance (REDOR) NMR (11).

We first characterized the temperature dependence of the <sup>31</sup>P signal using single pulse excitation and cross polarization. Single pulse excitation yields the most intense signals for mobile sites in MAS experiments, while cross polarization yields signals only for immobile sites. Using MAS, a well-resolved <sup>31</sup>P NMR resonance was observed with single pulse excitation until the sample temperature reached –40 °C. Below this temperature, the resonance broadened and was only observed using cross polarization. These results indicate that the C-terminus is highly mobile above –40 °C and immobilized at lower temperature. Rotational-echo double-resonance (REDOR) techniques were then used to measure the internuclear distance between the <sup>31</sup>P-label on the C-terminal tail and the <sup>19</sup>F-labels on Cys140 and Cys316. The heteronuclear distance measurements indicate that the <sup>19</sup>F...<sup>31</sup>P distances are all greater than 12 Å. These results

<sup>1</sup> Abbreviations: EPR, electron paramagnetic resonance; DM, dodecylmaltoside; GPCR, G protein-coupled receptor; MAS, magic angle spinning; NMR, nuclear magnetic resonance; OG, octyl-β glucoside; REDOR, rotational-echo double-resonance; 4-PDS, 4'-dithiopyridine; TET, 2,2,2-trifluoroethanethiol; Pi, inorganic phosphate; WT, wild-type.

show that the phosphorylated rhodopsin C-terminus does not contact the two areas in the cytoplasmic domain implicated for the interaction with arrestin. This implies that there is a change in the average position of the C-terminal tail upon phosphorylation from that observed in the crystal structure of the unphosphorylated receptor.

## MATERIALS AND METHODS

Frozen retinas were purchased from J. A. Lawson Co. (Lincoln, NE). 11-*cis*-Retinal was prepared from all-*trans*-retinal according to a published procedure (12). 4,4'-Dithiopyridine (4-PDS) (Sigma, St. Louis, MO), 2,2,2-trifluoroethanethiol (TET) (Aldrich), dodecylmaltoside (DM), and octyl- $\beta$  glucoside (OG) (Anatrace, Maumee, OH) were used without further purification. Antirhodopsin monoclonal antibody 1D4 was purified from a myeloma cell line provided by R. S. Molday (University of British Columbia). It was coupled to cyanogen bromide-activated Sepharose 4B (Sigma St. Louis, MO) as described previously (13), at a level of  $\sim 10$  mg/mL of swollen Sepharose beads. The antibody epitope, a nonapeptide corresponding to the C-terminal sequence of rhodopsin, was prepared by the Biopolymers Laboratory at the Massachusetts Institute of Technology.

Buffers used were as follows: buffer A, 20 mM 1,3-bis-[tris(hydroxymethyl) methylamino]propane (BTP) (pH 6.0); buffer B, 20 mM BTP, 2 mM MgCl<sub>2</sub>, 3 mM ATP (100–1000 cpm/pmol) (pH 7.5); buffer C, buffer A + 1% DM; buffer D, buffer A + 0.05% DM; buffer E, 20 mM BTP (pH 6.0) in 99.9% D<sub>2</sub>O (Cambridge Isotopes, Andover, MA); buffer F, 40 mM PIPES, 2 mM MgCl<sub>2</sub>, 2 mM CaCl<sub>2</sub>, 0.2 mM EDTA, 0.3 M NaCl, 0.05% DM (pH 6.5); buffer G, 2 mM NaH<sub>2</sub>PO<sub>4</sub>/Na<sub>2</sub>HPO<sub>4</sub>, 0.05% DM (pH 6.0); buffer H, buffer G + 0.3 M methyl- $\alpha$ -D-mannopyranoside.

*UV-Vis Absorption Spectroscopy.* UV-vis absorption spectra were recorded on a Perkin-Elmer  $\lambda 6$  spectrophotometer. The molar extinction value used for rhodopsin was 42 700 M<sup>-1</sup> cm<sup>-1</sup> (14).

*Time Course of Phosphorylation of Rhodopsin in ROS Membranes.* ROS membranes were prepared as described previously (15) and suspended in 5 mL of buffer B at a concentration of 0.5 mg/mL rhodopsin. 11-*cis*-Retinal (2 molar excess; final concentration 25  $\mu$ M) was added, and the suspension was sonicated for 1 min prior to initiation of the reaction by illumination. The reaction mixture was illuminated using light from a 300 W projector lamp at 15 cm with a  $<495$  nm cutoff filter at 20 °C, initially for 3 min and then for 2 min at 10 min intervals. Aliquots containing 0.25 mg of rhodopsin (500  $\mu$ L) were taken at 0, 10, 20, 30, 50, 70, and 90 min intervals, and EDTA was added to a final concentration of 20 mM to stop the reaction. The reaction mixture aliquots were centrifuged at 100 000g (Beckman 70 Ti) for 15 min at 4 °C, and ROS pellets were washed three times by homogenizing in 2 volumes (1 mL) of ice-cold buffer A, containing 20 mM EDTA, and centrifugation was repeated as stated previously. Finally, the pellets in the aliquots were resuspended in 500  $\mu$ L of buffer A, containing 11-*cis*-retinal (25  $\mu$ M), and regeneration of the chromophore was allowed overnight at 4 °C. The ROS membranes were then solubilized in 500  $\mu$ L of buffer C for 1 h at 4 °C. The supernatant was collected by centrifugation at 125 000g for 30 min at 4 °C. The extent of phosphorylation

by endogenous rhodopsin kinase was determined in each aliquot by taking a 50  $\mu$ L portion of the supernatant and Cerenkov counting of radioactivity. The rhodopsin concentration in the aliquots was determined by UV/vis difference spectra in the dark and after illumination. The bulk of the solubilized fractions ( $\sim 450$   $\mu$ L) were applied on 1D4 Sepharose (0.35 mL) columns, the flow-through being reapplied until all of the rhodopsin in the original samples in the dark was bound to the column. The columns were washed with 70 column volumes of buffer D, and rhodopsin was eluted by application of buffer D containing 100  $\mu$ M nonapeptide epitope. Fractions corresponding to 1 column volume were collected and analyzed by UV/vis absorbance and Cerenkov counting of residual <sup>32</sup>P radioactivity.

*Large Scale Preparation of Phosphorylated Wild-Type (WT) Rhodopsin.* ROS membranes, containing 30 mg of rhodopsin, were suspended in 60 mL of buffer B at a concentration of 0.5 mg/mL rhodopsin. 11-*cis*-Retinal (2 molar excess; 25  $\mu$ M final concentration) was added, and the reaction mixture was divided into three tubes of 20 mL each and subjected to phosphorylation separately in each tube. After sonication for several minutes, each tube was illuminated for 3 min initially and for 2 min at 10 min intervals for a total of 60 min using  $>495$  nm light at 20 °C from a 300 W projector lamp. An aliquot containing 0.25 mg (500  $\mu$ L) of rhodopsin was taken at 0 min as the dark control. Phosphorylation was terminated by the addition of EDTA to a concentration of 20 mM, and the reaction mixtures were centrifuged at 125 000g for 30 min at 4 °C. The ROS pellets were washed three times by homogenizing in 2 volumes (40 mL/each tube) of ice-cold buffer A, containing 20 mM EDTA, and were centrifuged at 125 000g for 30 min at 4 °C. Regeneration with 2-fold molar excess of 11-*cis*-retinal (25  $\mu$ M) was performed overnight at 4 °C in 60 mL of buffer A for each of the three tubes.

*TET-Labeling of Cys316 and Cys140 in Phosphorylated WT Rhodopsin.* TET-labeling of phosphorylated rhodopsin was performed as described (10). Briefly, pelleted ROS membranes that were phosphorylated as described previously were resuspended in 60 mL of buffer A to a final concentration of 0.5 mg/mL of rhodopsin. 4-PDS was added to a final concentration of 1 mM, and the mixture was nutated end-over-end for 3 h at room temperature in the dark. Excess 4-PDS was removed by centrifugation at 35 000 rpm (Beckman 70 Ti) for 30 min at 4 °C. The pellet was resuspended in 30 mL of buffer A to a final concentration of 1 mg/mL rhodopsin, and TET was added to a final concentration of 1 mM. The reaction was allowed to proceed overnight at 4 °C with end-over-end nutation. Excess TET was removed by centrifugation at 125 000g for 30 min at 4 °C.

*Immunoaffinity Purification of Phosphorylated TET-Labeled WT Rhodopsin on 1D4 Sepharose.* The TET-labeled phosphorylated ROS pellet containing 30 mg of rhodopsin was solubilized in 30 mL of buffer C for 1 h at 4 °C. Binding to 30 mL of 1D4 Sepharose was performed by an application of the total solution overnight at 4 °C, and the column was washed with 100 column volumes of buffer D. Rhodopsin was eluted with buffer D containing 100  $\mu$ M nonapeptide epitope. Fractions corresponding to 1 column volume were collected and analyzed by UV/vis absorbance and Cerenkov counting of radioactivity.

*Immunoaffinity Purification of Phosphorylated TET-Labeled WT Rhodopsin on ConA Sepharose.* The TET-labeled phosphorylated ROS pellet containing 5 mg of rhodopsin was solubilized in 5 mL of buffer C for 1 h at 4 °C. Purification was accomplished by binding the solubilized pellet to a 3 mL column of ConA-Sepharose in buffer F; the column was then washed with 50 column volumes of buffer F and 10 column volumes of buffer G. Rhodopsin was eluted by application of buffer H. Fractions of 1 column volume were collected and analyzed by absorbance spectroscopy.

*Large Scale Preparation of WT Rhodopsin Reconstituted with 14,15-<sup>13</sup>C Retinal.* Wild-type rhodopsin for the <sup>13</sup>C NMR experiments demonstrating metarhodopsin II trapping was expressed in HEK293S cells and purified as described previously (16). A 2-fold molar excess (25 μM) of 14,15-<sup>13</sup>C 11-*cis*-retinal synthesized by standard methods (17) was added to DM-solubilized rhodopsin. The sample was illuminated for 2 min using >495 nm light at 20 °C from a 300 W projector lamp, and regeneration with 14,15-<sup>13</sup>C 11-*cis*-retinal occurred overnight at 4 °C. No further purification was needed due to the large difference in chemical shift of the 14 and 15 carbons between bound and free retinal.

*Illumination of Concentrated WT Rhodopsin and Determination of Metarhodopsin II Decay.* Purified rhodopsin in DM (10 mg in ~100 μL) was placed on ice and illuminated with a 300 W projector lamp using a >495 nm cutoff filter. Aliquots of 1 μL were taken at 0 s, 30 s, and 1 min and diluted to 400 μL with buffer G. As determined by UV/vis spectroscopy, bleaching to form metarhodopsin II was completed within 30 s. For measuring the decay of metarhodopsin II, aliquots of 1 μL were taken at 0 min, 15 min, 30 min, 1 h, 2 h and 4 min, 3 h and 5 min, 5 h and 22 min, 6 h and 18 min, and 48 h after illumination and diluted to 400 μL with buffer G. The samples were treated with 2 μL of 2 N H<sub>2</sub>SO<sub>4</sub>, and the absorption at 440 nm was recorded after 2 min.

*Solution State NMR Sample Preparation.* Fractions obtained after elution from 1D4 Sepharose and ConA Sepharose with ratios ( $A_{280}/A_{500}$ ) of 1.6–1.7 were collected and concentrated by using Centricon-30 filters. This resulted in an increase of the DM concentration from 0.05 to 4–7%. The buffer was exchanged to buffer E as described (10). Approximately 15 mg of rhodopsin in 350 μL was analyzed at 20 °C by solution NMR.

*Solid State NMR Sample Preparation.* For MAS NMR, 12.5 mg (<sup>31</sup>P experiments) and 5 mg (<sup>13</sup>C experiments) of rhodopsin solubilized in DM was concentrated under a stream of argon for 2–3 h at 20 °C to a volume no greater than 100 μL. The samples were transferred into NMR rotors by centrifugation at 3400 rpm for 2 min at 4 °C using a homemade unit. No more than a 10% loss of the sample was observed during a control experiment with ROS rhodopsin.

*Illumination of Phosphorylated TET-Labeled WT Rhodopsin.* Phosphorylated TET-labeled WT rhodopsin concentrate (~10 mg in ~100 μL) was prepared as stated previously for transfer to an NMR sample rotor for MAS experiments. The sample was illuminated on ice for 30 s using a 400 W source with a 500 nm high pass filter and immediately transferred into a cold probe (–110 °C). As a result, the

sample temperature never exceeded ~4 °C after illumination for more than 2 min.

*NMR Spectroscopy. Solution NMR.* Solution <sup>19</sup>F and <sup>31</sup>P NMR spectra were recorded on a Varian INOVA 501 spectrometer at 20 °C. Data acquisition and analysis were carried out using VNMR Version 6.1 software. Spectra were referenced to external trifluoroacetate for <sup>19</sup>F and sodium phosphate buffer for <sup>31</sup>P. The acquisition time was 24–30 h.

*Solid State NMR.* Solid state <sup>13</sup>C and <sup>31</sup>P MAS NMR spectra were recorded on Bruker Avance 600 and 360 MHz NMR spectrometers, respectively. Data acquisition and analysis were carried out using XWINNMR software. Samples were referenced to external TMS for <sup>13</sup>C and to ammonium diphosphate for <sup>31</sup>P. The <sup>13</sup>C spectra of 14,15-<sup>13</sup>C rhodopsin and metarhodopsin II were obtained with 11 kHz MAS using <sup>1</sup>H-<sup>13</sup>C cross polarization. The sample temperature was maintained at –80 °C for both the rhodopsin and the metarhodopsin II <sup>13</sup>C experiments.

A series of <sup>31</sup>P NMR spectra (4000 scans each) was obtained of rhodopsin as a function of temperature from 0 to –50 °C using single pulse excitation and high power proton decoupling during acquisition. <sup>1</sup>H-<sup>31</sup>P cross polarization was used to observe <sup>31</sup>P at –110 °C for the rhodopsin and metarhodopsin II after 48 000 scans.

REDOR experiments were used to observe <sup>31</sup>P-<sup>19</sup>F dipolar couplings in rhodopsin and metarhodopsin II. The <sup>31</sup>P-observed REDOR pulse sequence uses a train of <sup>19</sup>F π pulses with two pulses per rotor cycle. A single <sup>31</sup>P π pulse was used to refocus the chemical shift interaction. REDOR experiments were carried out with 5 kHz MAS and 60 rotor cycles of dephasing pulses, corresponding to a 12 ms dephasing time. Acquisition of the full *S*<sub>0</sub> and dephased *S* spectra were interleaved to help compensate for long-term spectrometer drift. The normalized echo differences, Δ*S*/*S*<sub>0</sub>, for these two experiments were analyzed using a Mathematica program kindly provided by Terry Gullion (West Virginia University).

## RESULTS

*Phosphorylation of WT Rhodopsin.* The aim was to introduce a single phosphate group per rhodopsin molecule. Phosphorylation of rhodopsin by rhodopsin kinase occurs at up to seven serines and threonines at the C-terminus of rhodopsin depending on the conditions used (18) but predominantly at two sites, Ser 338 and Ser 343 (Figure 1) (1, 2). The time course of phosphorylation of rhodopsin in ROS membranes observed under the conditions described in the Materials and Methods is shown in Figure 2A (upper curve, ▲), yielding a maximum level of 1.5 mol of phosphate/mol of rhodopsin. Purification of aliquots taken at different intervals by passage through 1D4-Sepharose gave the values plotted in the lower curve (●) of Figure 2A. The final level of phosphorylation was 0.8 mol of phosphate/mol of rhodopsin. Passage through 1D4-Sepharose was required to reduce the number of rhodopsin species phosphorylated at different positions (see below). The conditions determined in a small scale experiment were applied for the large scale (30 mg of rhodopsin) phosphorylation.

*TET-Labeling of Cysteines 140 and 316 in Phosphorylated Rhodopsin.* Phosphorylated rhodopsin was derivatized with

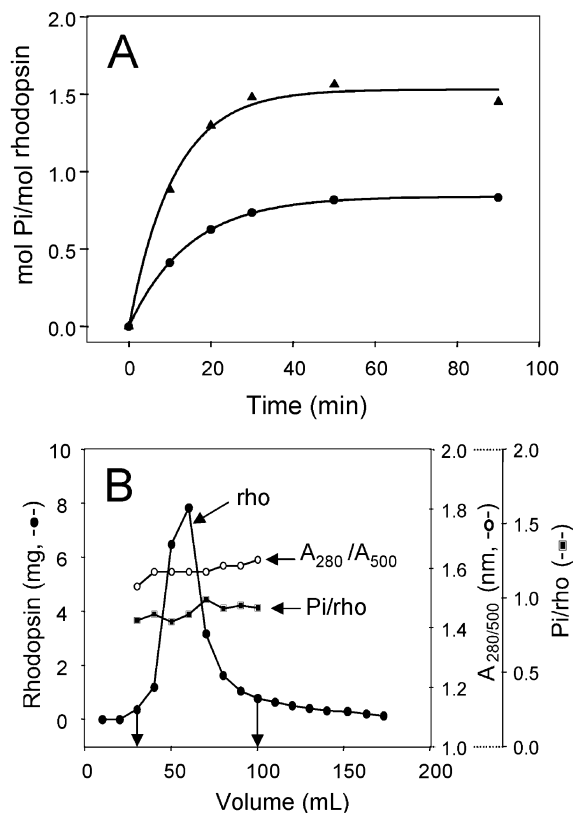


FIGURE 2: Preparation and purification of phosphorylated and TET-labeled (Cys140, 316) rhodopsin. (A) Time course of phosphorylation of rhodopsin in ROS membranes. Phosphorylation was performed in intact ROS by endogenous rhodopsin kinase (Materials and Methods) at 20 °C in the presence of a 2-fold excess of 11-*cis*-retinal. Aliquots were taken at time intervals, and the extent of phosphorylation was determined in membranes (▲). Aliquots of the membrane suspension removed at intervals were purified by passage through 1D4 Sepharose, and the extent of phosphorylation was determined (●). (B) Large scale purification of phosphorylated and TET-labeled (Cys140, 316) rhodopsin. Phosphorylation of rhodopsin in ROS membranes was performed using 30 mg of rhodopsin. Following reconstitution with 11-*cis*-retinal, the phosphorylated products were derivatized at Cys140 and Cys316 with TET groups. The resulting phosphorylated and TET-labeled rhodopsin was purified on an antibody 1D4-Sepharose column (Materials and Methods). The elution profile of rhodopsin from the column (mg) (●),  $A_{280}/A_{500}$  (○), and Pi/rhodopsin ratios (■) in eluted fractions are shown.

TET as described in the Materials and Methods to give TET-labeled phosphorylated rhodopsin. The total product was applied to a 30 mL 1D4-Sepharose column. The elution profile is shown in Figure 2B. The rhodopsin content,  $A_{280}/A_{500}$  ratio, and the Pi/rhodopsin ratio in the different column fractions are plotted in Figure 2B. About 25 mg of the product with a  $A_{280}/A_{500}$  ratio of  $\sim 1.6$  was obtained on pooling the fractions between the arrows.

**Solution  $^{31}\text{P}$  NMR Spectra in the Dark of the TET-Labeled Phosphorylated WT Rhodopsin.** The  $^{31}\text{P}$  NMR spectrum in the dark of TET-labeled phosphorylated rhodopsin purified as described previously is shown in Figure 3A. The major phosphate peak observed was at 2.2 ppm, and a second minor peak was observed upfield of the major phosphate peak. This high level of homogeneity was only obtained after passage of the sample through 1D4-Sepharose (see above). When phosphorylated rhodopsin was purified by ConA-sepharose, which binds to the N-terminus of rhodopsin, significantly

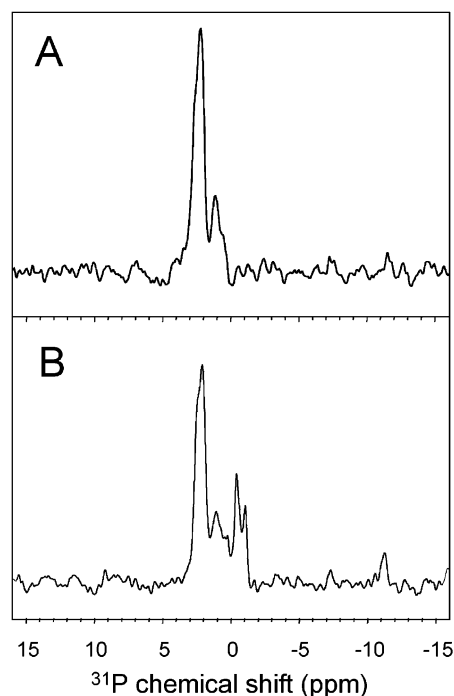


FIGURE 3:  $^{31}\text{P}$  NMR solution spectra in the dark of phosphorylated TET-labeled WT rhodopsin. Approximately 5 and 4.5 mg of phosphorylated TET-labeled rhodopsin were purified, respectively, on 1D4 Sepharose (as in Figure 2) and on ConA Sepharose (Materials and Methods). The samples were analyzed by solution NMR (15 000 scans) at 20 °C. (A) Spectrum of 1D4-Sepharose purified sample and (B) spectrum of ConA-Sepharose purified sample; the spectra were referenced to 2 mM sodium phosphate buffer as an external standard (Materials and Methods).

more heterogeneity was observed, as shown by the  $^{31}\text{P}$ -solution NMR spectrum in Figure 3B. While the main peak is identical to that seen for the 1D4-Sepharose-purified sample (Figure 3A), there are numerous minor peaks upfield of this resonance. Thus, immunoaffinity purification on 1D4-Sepharose had removed the majority of the minor polyphosphorylated rhodopsin species and resulted in an overall lower level of phosphorylation. This is due to the fact that Thr342 has been shown to be important in binding to the antibody 1D4, and phosphorylation at or near this site (Ser 343) may be expected to result in nonbinding of such species. Furthermore, the presence of multiple phosphate groups at the C-terminus has previously been found to strongly affect binding to the 1D4 antibody (19). Phosphorylation at the other preferred phosphorylation site, Ser338, will not affect binding of rhodopsin to 1D4-Sepharose; therefore, we deduce that the main peak observed in Figure 3A corresponds to rhodopsin phosphorylated at this position.

**Solution  $^{19}\text{F}$  NMR Spectra in the Dark of the TET-Labeled Phosphorylated WT Rhodopsin.**  $^{19}\text{F}$  NMR spectra (Figure 4) of TET-labeled phosphorylated rhodopsin in DM exhibited two resolved resonances at 10.6 and 10.05 ppm, which were previously assigned to Cys140 and Cys316, respectively (10). A downfield shift was observed in the Cys140 resonance from 10.6 to 10.25 ppm with a change of detergent from DM to OG as described previously (10). No change in the chemical shift of Cys316 was detected, which suggests that Cys316 faces the solution and is not influenced by the nature of detergent. The spectra clearly show that the protein is TET-labeled at both cysteine sites.

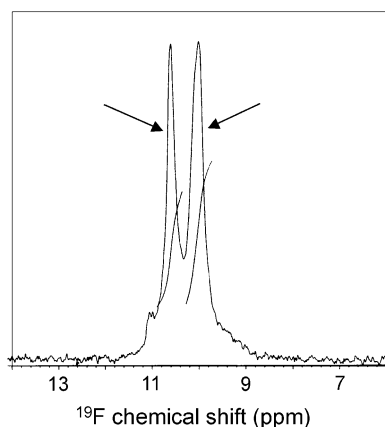


FIGURE 4:  $^{19}\text{F}$  NMR solution spectra of phosphorylated  $^{19}\text{F}$ -labeled WT rhodopsin in the dark. NMR spectra in  $\sim 4\%$  DM at room temperature were obtained of  $\sim 15$  mg of phosphorylated TET-labeled WT rhodopsin purified by 1D4 affinity chromatography.

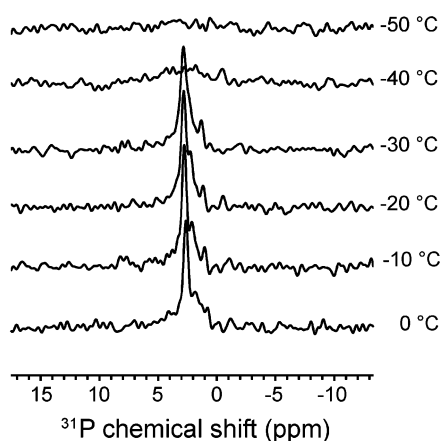


FIGURE 5:  $^{31}\text{P}$  MAS NMR spectra of phosphorylated WT rhodopsin in the dark obtained with single pulse excitation as a function of temperature (Materials and Methods). The MAS frequency was maintained at 5000 Hz, and the sample temperature was varied from 0 to  $-50$   $^{\circ}\text{C}$ .

*$^{31}\text{P}$ -MAS NMR Spectra in the Dark of the TET-Labeled Phosphorylated WT Rhodopsin.* Figure 5 presents a series of  $^{31}\text{P}$  spectra of phosphorylated WT rhodopsin obtained as a function of temperature. The  $^{31}\text{P}$  spectrum at  $0$   $^{\circ}\text{C}$  exhibits a single intense  $^{31}\text{P}$  resonance at 2.5 ppm as well as several weaker resonances between 0.5 and 2 ppm. The  $^{31}\text{P}$  line width increases slightly as the temperature decreases to  $-40$   $^{\circ}\text{C}$ . At this temperature, the  $^{31}\text{P}$  resonance broadens to a line width of  $>5$  ppm. This broadening is interpreted as a loss of mobility of the C-terminal tail.

The spectra shown in Figure 5 were all obtained using a simple single pulse experiment. The single  $^{31}\text{P}$  pulse excites nuclei associated with both mobile and nonmobile sites. For comparison, excitation with  $^1\text{H}$ - $^{31}\text{P}$  cross polarization, which is sensitive to only nuclei in nonmobile sites, did not yield a  $^{31}\text{P}$  signal until the temperature was at or below  $-40$   $^{\circ}\text{C}$  (data not shown). The loss of intensity above  $-40$   $^{\circ}\text{C}$  is consistent with increased mobility of the C-terminal tail, while the broadened line width below  $-40$   $^{\circ}\text{C}$  is consistent with the C-terminal tail being immobilized in a number of conformations.

*$^{31}\text{P}$ -Observed,  $^{19}\text{F}$ -Dephased REDOR NMR Spectra of TET-Labeled Phosphorylated WT Rhodopsin and Metarhodopsin II.* Measurement of the distance between the  $^{31}\text{P}$

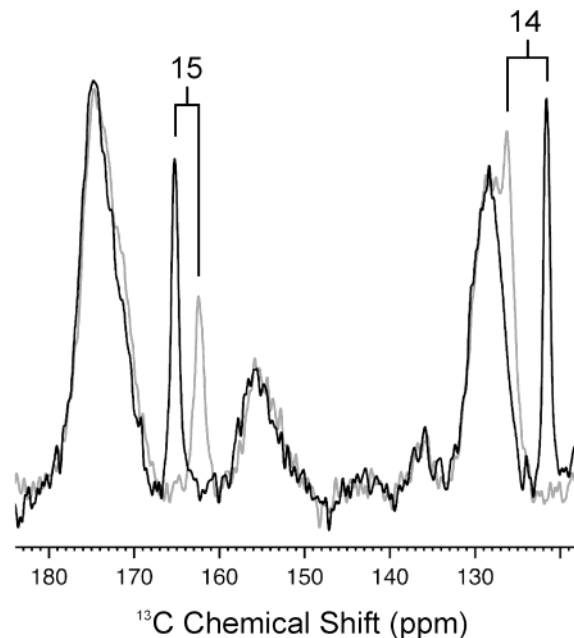


FIGURE 6:  $^{13}\text{C}$ -MAS NMR spectra of rhodopsin (black) and metarhodopsin II (gray) regenerated with  $14,15\text{-}^{13}\text{C}$  retinal. The chemical shifts of the  $14\text{-}^{13}\text{C}$  and  $15\text{-}^{13}\text{C}$  resonances of 126.3 and 162.4 ppm, respectively, in metarhodopsin II are characteristic of an all-*trans* unprotonated retinal Schiff base. The sample temperature was maintained at  $-80$   $^{\circ}\text{C}$  for the duration of the experiment, 5–7 days, without any loss of intensity or shift in the retinal resonances. These results demonstrate stable trapping of the metarhodopsin II intermediate in detergent micelles.

sites in the C-terminal tail and the  $^{19}\text{F}$  labels introduced into the cytoplasmic loops of rhodopsin was attempted using REDOR NMR for both dark- and light-activated rhodopsin (metarhodopsin II). For metarhodopsin II, the rhodopsin sample was illuminated on ice for 30 s (Materials and Methods) and transferred into the NMR probe and cooled to  $-110$   $^{\circ}\text{C}$ . This process took  $\sim 3$  min. To determine the efficiency of metarhodopsin II trapping in the NMR sample, two separate experiments were performed. First, absorption spectra were recorded on a parallel sample as a function of time following illumination. The  $T_{1/2}$  of metarhodopsin II decay with the sample on ice was 306 min, as compared to 15 min at  $20$   $^{\circ}\text{C}$  (20) and 77 min at  $4$   $^{\circ}\text{C}$  (21). Therefore, after the time required for transfer of the sample to the rotor, more than 90% of metarhodopsin II was still present in the sample analyzed. Second, NMR data were obtained on a sample regenerated with  $14,15\text{-}^{13}\text{C}$  retinal in the dark and upon illumination. The  $14,15\text{-}^{13}\text{C}$  chemical shifts of the retinal are sensitive to the protonation state of the Schiff base and provide an internal control for whether metarhodopsin II can be stabilized at low temperature for the duration of the MAS NMR experiments. Figure 6 shows the  $^{13}\text{C}$  spectrum of rhodopsin (black) and metarhodopsin II (gray) solubilized in DM. The  $14,15\text{-}^{13}\text{C}$  chemical shifts are at 121.6 and 165.2 ppm in rhodopsin, respectively, and shift to 126.3 and 162.4 ppm upon illumination of the sample. The latter chemical shifts are characteristic of an unprotonated all-*trans*-retinal Schiff base, demonstrating trapping of the metarhodopsin II intermediate. Over an extended time course of 5–7 days, no changes in intensity or chemical shift were observed in the retinal resonances after conversion of the sample to the metarhodopsin II intermediate. Therefore, we

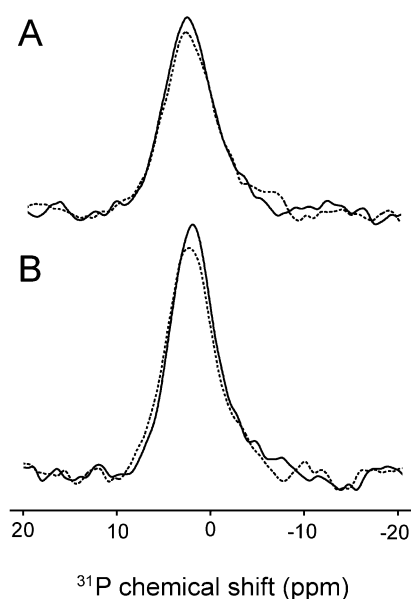


FIGURE 7:  $^{31}\text{P}$ -observed,  $^{19}\text{F}$ -dephased REDOR NMR spectra of rhodopsin in the dark (A) and upon light-activation (B). Under the conditions used, 90% of the light-activated sample corresponded to metarhodopsin II. The full REDOR  $S_0$  spectra are shown as solid lines, while the  $S$  spectra obtained with 60 rotor cycles of dephasing pulses are shown as dashed lines. The sample temperature was maintained at  $-110^\circ\text{C}$ , and the MAS frequency was maintained at 5000 Hz.

conclude that at less than  $-80^\circ\text{C}$ , the metarhodopsin II intermediate is stable.

The solid state NMR experiments differ from those previously reported (22, 23) using ROS membranes rather than detergent. The current study focuses on the phosphorylated C-terminus in both dark- and light-activated rhodopsin. Regeneration with 14,15- $^{13}\text{C}$  retinal in ROS membranes allowed us to quantify the formation and stability of metarhodopsin II. In ROS membranes, we were not able to obtain a homogeneous population of metarhodopsin II even at low pH. Moreover, the use of detergent greatly simplifies the  $^{31}\text{P}$  NMR spectrum, which only exhibits the resonances due to the phosphorylated sites on the C-terminus.

The  $^{31}\text{P}$ -observed REDOR experiment requires the acquisition of two spectra, a full echo spectrum,  $S_0$ , with no dephasing pulses on the  $^{19}\text{F}$  channel, and a dephased spectrum,  $S$ , resulting from the application of a train of  $^{19}\text{F}$  dephasing pulses. The intensity change ( $\Delta S$ ) between the two spectra is related to the dipolar coupling and hence the internuclear distance. In REDOR experiments on an isolated  $^{31}\text{P}\cdots^{19}\text{F}$  pair separated by 10 Å and using 60 rotor cycles of dephasing pulses and spinning at 5 kHz, one would calculate an intensity change ( $\Delta S$ ) of 30% (11). Figures 7A,B presents the  $S_0$  (solid line) and  $S$  (dashed line) REDOR spectra of rhodopsin and metarhodopsin II, respectively. The  $S$  spectra were obtained using 60 rotor cycles of dephasing pulses and a MAS frequency of 5 kHz. In both rhodopsin and metarhodopsin II, the intensity difference between the  $S_0$  and the  $S$  spectra is less than 10%, which corresponds to an average  $^{31}\text{P}\cdots^{19}\text{F}$  distance of greater than 12 Å.

## DISCUSSION

Phosphorylation of the C-terminus of rhodopsin is a key step in its inactivation. Binding of arrestin to the cytoplasmic

surface of rhodopsin as a result of C-terminal phosphorylation blocks the binding and activation of the heterotrimeric G protein, transducin. As a result, establishing the location and mobility of the phosphorylated C-terminal tail of rhodopsin is essential for understanding the first step in the inactivation process. The crystal structure of rhodopsin provides information on the structure of the C-terminal tail in the unphosphorylated state. The crystal structure shows that the C-terminus folds back toward the center of the helical bundle bringing the two major phosphorylation sites, Ser338 and Ser343, into close proximity with the tertiary structure formed by helix 8, the ends of helices 1 and 2 and their connecting loop. In particular, Cys316 on helix 8 interacts closely with His65 in the first cytoplasmic loop and with Asn73 at the end of helix 2. The crystal structure places Ser338, the site of phosphorylation investigated in the present study, within 4–5 Å of Cys316 in helix 8 (Figure 1) (6, 7).

To test if the phosphate ( $^{31}\text{P}$ ) group at position Ser338 is in close proximity to Cys316, we measured the distance to the  $^{19}\text{F}$  label attached to Cys316 using REDOR NMR. The lack of dephasing indicates that the average  $^{31}\text{P}$ - $^{19}\text{F}$  distance is greater than 12 Å. This result clearly demonstrates that the conformation observed in the crystal structure is no longer maintained upon phosphorylation. Taken together, the increased mobility, broader line widths at low temperature, and the long average  $^{31}\text{P}$ - $^{19}\text{F}$  distance suggest that the C-terminal tail becomes disordered upon phosphorylation and that we are probing a heterogeneous conformation of the phosphorylated C-terminal tail in the REDOR experiments. The REDOR experiment also measures the distance between the C-terminal phosphates and the  $^{19}\text{F}$  label at Cys140. Again, the lack of significant dephasing indicates an average  $^{31}\text{P}$ - $^{19}\text{F}$  distance of greater than 12 Å. The disorder and mobility of the C-terminal tail in phosphorylated rhodopsin are consistent with previous  $^{31}\text{P}$  MAS NMR studies in ROS membranes (22, 23).

Rhodopsin kinase is not able to phosphorylate rhodopsin in its dark, inactive state. The position of the phosphorylation sites in the C-terminal tail in the crystal structure of rhodopsin is consistent with these sites not being accessible to rhodopsin kinase. Moreover, in unphosphorylated rhodopsin, the C-terminal tail interacts with the cytoplasmic loops and blocks the critical sites involved in arrestin binding, Asn73, Pro142, and Met143. Upon activation of rhodopsin and phosphorylation of Ser338 and Ser343, the C-terminal tail becomes mobile and is able to interact with and activate arrestin. The observation that the C-terminal tail of phosphorylated rhodopsin in the dark, inactive state is also mobile and unstructured suggests that the conformational changes upon light absorption are necessary for exposing the phosphorylation sites to rhodopsin kinase but that phosphorylation alone is all that is needed to free the C-terminal tail to interact with arrestin.

## REFERENCES

- Ohguro, H., Palczewski, K., Ericsson, L. H., Walsh, K. A., and Johnson, R. S. (1993) Sequential phosphorylation of rhodopsin at multiple sites, *Biochemistry* 32, 5718–24.
- Ohguro, H., Rudnicka-Nawrot, M., Buczylo, J., Zhao, X., Taylor, J. A., Walsh, K. A., and Palczewski, K. (1996) Structural and enzymatic aspects of rhodopsin phosphorylation, *J. Biol. Chem.* 271, 5215–24.

3. McDowell, J. H., Nawrocki, J. P., and Hargrave, P. A. (1993) Phosphorylation sites in bovine rhodopsin, *Biochemistry* 32, 4968–74.
4. Raman, D., Osawa, S., and Weiss, E. R. (1999) Binding of arrestin to cytoplasmic loop mutants of bovine rhodopsin, *Biochemistry* 38, 5117–23.
5. Celver, J., Vishnivetskiy, S. A., Chavkin, C., and Gurevich, V. V. (2002) Conservation of the phosphate-sensitive elements in the arrestin family of proteins, *J. Biol. Chem.* 277, 9043–8.
6. Palczewski, K., Kumasaka, T., Hori, T., Behnke, C. A., Motoshima, H., Fox, B. A., Le Trong, I., Teller, D. C., Okada, T., Stenkamp, R. E., Yamamoto, M., and Miyano, M. (2000) Crystal structure of rhodopsin: A G protein-coupled receptor, *Science* 289, 739–45.
7. Okada, T., Fujiyoshi, Y., Silow, M., Navarro, J., Landau, E. M., and Shichida, Y. (2002) Functional role of internal water molecules in rhodopsin revealed by X-ray crystallography, *Proc. Natl. Acad. Sci. U.S.A.* 99, 5982–7.
8. Klein-Seetharaman, J., Reeves, P. J., Loewen, M. C., Getmanova, E. V., Chung, J., Schwalbe, H., Wright, P. E., and Khorana, H. G. (2002) Solution NMR spectroscopy of [ $\alpha$ - $^{15}\text{N}$ ]lysine-labeled rhodopsin: The single peak observed in both conventional and TROSY-type HSQC spectra is ascribed to Lys-339 in the carboxyl-terminal peptide sequence, *Proc. Natl. Acad. Sci. U.S.A.* 99, 3452–7.
9. Klein-Seetharaman, J., Hwa, J., Cai, K. W., Altenbach, C., Hubbell, W. L., and Khorana, H. G. (2001) Probing the dark state tertiary structure in the cytoplasmic domain of rhodopsin: Proximities between amino acids deduced from spontaneous disulfide bond formation between Cys316 and engineered cysteines in cytoplasmic loop I, *Biochemistry* 40, 12472–8.
10. Klein-Seetharaman, J., Getmanova, E. V., Loewen, M. C., Reeves, P. J., and Khorana, H. G. (1999) NMR spectroscopy in studies of light-induced structural changes in mammalian rhodopsin: Applicability of solution F-19 NMR, *Proc. Natl. Acad. Sci. U.S.A.* 96, 13744–9.
11. Gullion, T., and Schaefer, J. (1989) Rotational-Echo Double-Resonance NMR, *J. Magn. Reson.* 81, 196–200.
12. Knowles, A., and Priestley, A. (1978) The preparation of 11-*cis*-retinal, *Vision Res.* 18, 115–6.
13. Oprian, D. D., Molday, R. S., Kaufman, R. J., and Khorana, H. G. (1987) Expression of a synthetic bovine rhodopsin gene in monkey kidney cells, *Proc. Natl. Acad. Sci. U.S.A.* 84, 8874–8.
14. Hong, K., and Hubbell, W. L. (1972) Preparation and properties of phospholipid bilayers containing rhodopsin, *Proc. Natl. Acad. Sci. U.S.A.* 69, 2617–21.
15. Molday, R. S., and MacKenzie, D. (1983) Monoclonal antibodies to rhodopsin: characterization, cross-reactivity, and application as structural probes, *Biochemistry* 22, 653–60.
16. Eilers, M., Reeves, P. J., Ying, W., Khorana, H. G. and Smith, S. O. (1999) Magic angle spinning NMR of the protonated retinylidene Schiff base nitrogen in rhodopsin: Expression of  $^{15}\text{N}$ -lysine- and  $^{13}\text{C}$ -glycine-labeled opsin in a stable cell line, *Proc. Natl. Acad. Sci. U.S.A.* 96, 487–92.
17. Lugtenburg, J. (1985) The synthesis of carbon-13 labeled retinals, *Pure Appl. Chem.* 57, 753–62.
18. Wilden, U., and Kuhn, H. (1982) Light-dependent phosphorylation of rhodopsin: number of phosphorylation sites, *Biochemistry* 21, 3014–22.
19. Molday, R. S., and MacKenzie, D. (1985) Inhibition of monoclonal antibody binding and proteolysis by light-induced phosphorylation of rhodopsin, *Biochemistry* 24, 776–81.
20. Farrens, D. L., and Khorana, H. G. (1995) Structure and function in rhodopsin. Measurement of the rate of metarhodopsin II decay by fluorescence spectroscopy, *J. Biol. Chem.* 270, 5073–6.
21. Klein-Seetharaman, J., Hwa, J., Cai, K., Altenbach, C., Hubbell, W. L., and Khorana, H. G. (1999) Single-cysteine substitution mutants at amino acid positions 55–75, the sequence connecting the cytoplasmic ends of helices I and II in rhodopsin: Reactivity of the sulfhydryl groups and their derivatives identifies a tertiary structure that changes upon light-activation, *Biochemistry* 38, 7938–44.
22. Albert, A. D., Frye, J. S., and Yeagle, P. L. (1990) Light-induced membrane protein phosphorylation in the bovine rod outer segment. A magic angle spinning  $^{31}\text{P}$  NMR study, *Biophys. Chem.* 36, 27–31.
23. Albert, A. D., Watts, A., Spooner, P., Groebner, G., Young, J., and Yeagle, P. L. (1997) A distance measurement between specific sites on the cytoplasmic surface of bovine rhodopsin in rod outer segment disk membranes, *Biochim. Biophys. Acta* 1328, 74–82.

BI030120U